Sliding Mode Control for Maximum Power Point Tracking of Photovoltaic Inverters in Microgrids

Michele Cucuzzella, Gian Paolo Incremona, Mauro Guastalli and Antonella Ferrara

***Abstract*— In this paper the design of sliding mode controllers for Maximum Power Point Tracking (MPPT) of a photovoltaic inverter in microgrids is presented. A master-slave configuration of the microgrid is considered in islanded operation mode where the photovoltaic Distributed Generation unit (DGu) serves as a slave. The DGu is also affected by nonlinearities, parameters and modelling uncertainties, which make the use of the sliding mode control methodology particularly appropriate. Specifically, a sliding mode controller, relying on the so-called unit vector approach, is first proposed to control the photovoltaic inverter. Then, a Second Order Sliding Mode (SOSM) controller, adopting a Suboptimal SOSM algorithm, is proposed to alleviate the chattering phenomenon and feed a continuos modulating signal into the photovoltaic inverter. Simulation tests, carried out on a realistic scenario, confirm satisfactory closed-loop performance of the proposed control scheme.**

I. Introduction

Photovoltaic (PV) arrays are able to generate electric power directly from sunlight, thus powering electrical devices or sending electric power to the main grid. Moreover, PV arrays represent one of the most used Renewable Energy Sources (RES) which have given rise to the new concept of microgrids, consisting of a certain number of Distributed Generation units (DGus) [1]. The development of this new paradigm could be very significant from technical, economical and environmental viewpoints, also improving the service quality both in grid-connected operation mode (GCOM) and even after the disconnection from the main grid, that is in the so-called islanded operation mode (IOM) [2].

Because of the unpredictable and uncertain nature of the meteorological agents, the problem to stabilize RES-based microgrids is an open problem. In the literature, conventional PI controllers are generally proposed to stabilize DGus [3], but the introduction of robust control strategies seems mandatory.

An other important issue in the context of PV-based microgrids is the possibility to track the maximum power point depending on the actual solar irradiation. In the literature, the so-called Maximum Power Point Tracking (MPPT) control has been considered [4], [5]. Specifically, there exist several approaches to solve this control problem, such as Pertube and Observe (P&O) method, the Incremental Conductance (IC) method, and the so-called Constant Voltage (CV) approach. Moreover, robust sliding mode based MPPT control scheme for three-phase grid-connected photovoltaic systems are proposed in [6], [7].

Sliding mode (SM) control [8], [9] is very appreciated for its robustness properties in front of the so-called matched disturbances, i.e., uncertain terms which act on the same channel of the control variable. SM control represents also an easy to implement solution. Yet, its discontinuous control laws can cause the so-called chattering problem, i.e., high frequency oscillations of the controlled variable due to the discontinuities of the input signal fed into the plant. In the literature, possible solutions to alleviate chattering are those based on the so-called higher order sliding mode (HOSM) [10]–[12], or on advanced SM control algorithms of adaptive, switching and event-triggered type [13]–[17].

In this paper, a master-slave architecture for PV-based microgrids in IOM is considered and robust sliding mode controllers, based on CV approach, are designed for the inverter of the PV DGu in order to track the maximum power point. In the paper an appropriate model of the PV DGu is introduced, along with a semplified model of the dynamics of an Energy Storage unit (ESu). Specifically, a first order sliding mode control based on the so-called unit vector approach [8] is designed for the MPPT of the PV DGu. Then, a Second Order Sliding Mode (SOSM) algorithm [18], [19] is proposed to guarantee good properties in terms of chattering alleviation and stability performance. Note that, the SOSM algorithm allows one to feed a continuos modulating signal into the photovoltaic inverter, which is based on the pulse width modulation (PWM) technique. The proposed control scheme is theoretically analyzed proving the robustness of the controlled system in spite of parameters variations, nonlinearities and modelling uncertainties. Finally, simulation results are presented relying on realistic scenarios of a PV-based microgrid.

The present paper is organized as follows. In Section II a PV-based microgrid is described, while in Section III the control problem is formulated. The master-slave architecture in IOM with the proposed controllers are presented in Section IV. In Section V, the proposed control scheme is theoretically analyzed, while simulation assessment is discussed in Section VI. Some conclusions are gathered in Section VII.

II. Preliminaries

Some preliminary issues on a typical photovoltaic-based microgrid are hereafter reported and the main operation modes

This is the final version of the accepted paper submitted to Proc. of 55th IEEE Conference on Decision and Control, Las Vegas, Dec. 2016. Work supported by EU Project ITEAM (project reference: 675999).
M. Cucuzzella, M. Guastalli and A. Ferrara are with the Dipartimento di Ingegneria Industriale e dell'Informazione, University of Pavia, via Ferrata 5, 27100 Pavia, Italy (e-mail: {michele.cucuzzella, mauro.guastalli01}@gmail.com, antonella.ferrara@unipv.it).

G. P. Incremona is with the Dipartimento di Ingegneria Civile e Architettura, University of Pavia, Via Ferrata 3, 27100 Pavia, Italy (e-mail: gp.incremona@gmail.com).

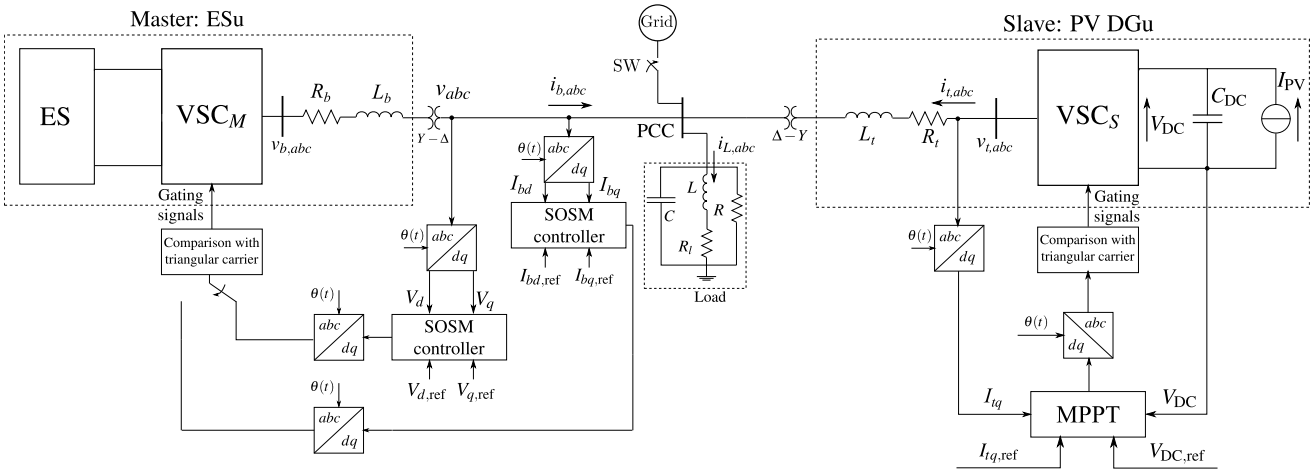

Fig. 1. Simplified schematic diagram of the considered microgrid with the photovoltaic DGu.

TABLE I
ELECTRICAL PARAMETERS OF THE DGU IN FIG. 1

Quantity	Value	Description
f_c	10 kHz	PWM carrier frequency
$R_t = R_b$	40 mΩ	Filter resistance
$L_t = L_b$	10 mH	Filter inductance
C_{DC}	0.01 F	DC-link capacity
R	4.33 Ω	Load resistance
L	100 mH	Load inductance
R_l	0.6 Ω	Parasitic resistance
C	1 pF	Load capacity
f_0	60 Hz	Grid frequency
V_n	120 V	Grid phase-voltage (RMS)

are briefly described.

A. The Photovoltaic-Based Microgrid

Consider the schematic representation in Fig. 1 of a typical microgrid with a photovoltaic (PV) DGu and an Energy Storage unit (ESu) in a typical master-slave configuration. Specifically, in IOM, the ESu serves as master and it provides a suitable current to the shared three-phase load, in order to keep the microgrid voltage constant to the nominal value. Note that, in this paper we assume that the ESu has an appropriate capacity to supply the microgrid loads. On the other hand, the PV DGu has the role of slave, tracking the maximum power point depending on the solar irradiation. PV arrays convert solar energy into direct current (DC) electric energy which is transformed into alternate current (AC) electric energy by a voltage-sourced-converter (VSC) with a pulse width modulation (PWM) technique. The VSC and the resistive-inductive (R_tL_t and R_bL_b) filter, able to extract the fundamental frequency of the inverter output voltage, are the interface medium with the point of common coupling (PCC), where a parallel resistive-inductive-capacitive (RLC) load is connected. Table I reports the parameters of the considered system.

B. The Operation Modes

When the PV-based microgrid works in GCOM, the PCC voltage amplitude and frequency are fixed by the grid. In order to decouple the control of the active and reactive power, a phase-locked-loop (PLL) steers to zero the quadrature voltage component V_q by using a proportional-integral (PI) controller. In such a case, the active and reactive power result equal to $P = 3/2V_dI_{td}$ and $Q = -3/2V_dI_{tq}$ respectively, where V_d is the direct component of load voltage v_{abc}, while I_{td}, I_{tq}, I_{bd}, I_{bq} are the direct and quadrature components of currents $i_{t,abc}$ and $i_{b,abc}$, respectively. Specifically, when ESu works in current control mode, it has to track the desired values P_{ref} and Q_{ref}, which depend only on I_{td} and I_{tq}, respectively.

On the other hand, the PV DGu is controlled such that the DC-link voltage V_{DC}, i.e., the voltage across the capacity C_{DC}, is held constant, so as to perform the Maximum (active) Power Point Tracking (MPPT). While, the generated reactive power is maintained equal to zero, by regulating $I_{tq} = 0$.

When the PV-based microgrid is disconnected from the main grid (that is the circuit breaker SW in Fig. 1 is open), the PCC voltage and frequency could be different with respect to the nominal values, due to the mismatch between the generated power and the load demand. Hence, in IOM the ESu switches from current control mode to voltage control mode and provides constant voltage in correspondence of the PCC, while the PV DGu is controlled in current control mode as in GCOM. Finally, an internal oscillator generates a constant angular frequency equal to the nominal one, namely $\omega_0 = 2\pi f_0$.

III. PROBLEM FORMULATION

A. Photovoltaic Distributed Generation Unit Model

Consider the scheme of the microgrid in Fig. 1, assuming the system to be symmetric and balanced. According to the stationary *abc*-frame, the governing equations for the PV

DGu are

$$\begin{cases} i_{t,abc} = \frac{1}{R} v_{abc} + i_{L,abc} + C\frac{dv_{abc}}{dt} \\ v_{abc} = L\frac{di_{L,abc}}{dt} + R_l i_{L,abc} \\ v_{t,abc} = L_t \frac{di_{t,abc}}{dt} + R_t i_{t,abc} + v_{abc} \\ I_{\mathrm{PV}} = C_{\mathrm{DC}} \frac{dv_{\mathrm{DC}}}{dt} + s_{abc}^T i_{t,abc} \end{cases} \tag{1}$$

where $i_{t,abc}$, $i_{L,abc}$, I_{PV}, v_{abc}, $v_{t,abc}$ and v_{DC} represent the currents delivered by the VSC, the currents fed into the load inductance (L), the DC current generated by PV arrays, the voltage of the PCC, the VSC output voltages and the DC-Link voltage, respectively, while s_{abc} are the command signals of the inverter switches, which can assume the value 1 (switch on) or the value 0 (switch off). Each phase signal in (1) can be written in the rotating dq-frame by applying the Clarke's and Park's transformations. Considering that

$$\begin{cases} S_d V_{\mathrm{DC}} = V_{td} \\ S_q V_{\mathrm{DC}} = V_{tq} \end{cases} \tag{2}$$

then, system (1) can be expressed as

$$\begin{cases} \dot{V}_d = -\frac{1}{RC} V_d + \omega_0 V_q - \frac{1}{C} I_{Ld} + \frac{1}{C} I_{td} \\ \dot{V}_q = -\omega_0 V_d - \frac{1}{RC} V_q - \frac{1}{C} I_{Lq} + \frac{1}{C} I_{tq} \\ \dot{I}_{Ld} = \frac{1}{L} V_d - \frac{R_l}{L} I_{Ld} + \omega_0 I_{Lq} \\ \dot{I}_{Lq} = \frac{1}{L} V_q - \omega_0 I_{Ld} - \frac{R_l}{L} I_{Lq} \\ \dot{I}_{td} = -\frac{1}{L_t} V_d - \frac{R_t}{L_t} I_{td} + \omega_0 I_{tq} + \frac{1}{L_t} V_{td} \\ \dot{I}_{tq} = -\frac{1}{L_t} V_q - \omega_0 I_{td} - \frac{R_t}{L_t} I_{tq} + \frac{1}{L_t} V_{tq} \\ \dot{V}_{\mathrm{DC}} = -\frac{3}{2} \frac{I_{td} V_{t,d}}{C_{\mathrm{DC}} V_{\mathrm{DC}}} - \frac{3}{2} \frac{I_{tq} V_{t,q}}{C_{\mathrm{DC}} V_{\mathrm{DC}}} + \frac{1}{C_{\mathrm{DC}}} I_{\mathrm{PV}} \end{cases} \tag{3}$$

The design of HOSM controllers for DGus in GCOM is described in detail in [20], [21]. For this reason, it is worth investigating the case in which the PV-based microgrid works in IOM, as will be described in the following subsections.

B. State-Space Representation

Consider the IOM case, when the ESu serves as master and the PV DGu has the role of slave. The equations which describe the dynamics of the overall system are the following

$$\begin{cases} \dot{V}_d = -\frac{1}{RC} V_d + \omega_0 V_q + \frac{1}{C} I_{bd} - \frac{1}{C} I_{Ld} + \frac{1}{C} I_{td} \\ \dot{V}_q = -\omega_0 V_d - \frac{1}{RC} V_q + \frac{1}{C} I_{bq} - \frac{1}{C} I_{Lq} + \frac{1}{C} I_{tq} \\ \dot{I}_{bd} = -\frac{1}{L_b} V_d - \frac{R_b}{L_b} I_{bd} + \omega_0 I_{bq} + \frac{1}{L_b} V_{bd} \\ \dot{I}_{bq} = -\frac{1}{L_b} V_q - \omega_0 I_{bd} - \frac{R_b}{L_b} I_{bq} + \frac{1}{L_b} V_{bq} \\ \dot{I}_{Ld} = \frac{1}{L} V_d - \frac{R_l}{L} I_{Ld} + \omega_0 I_{Lq} \\ \dot{I}_{Lq} = \frac{1}{L} V_q - \omega_0 I_{L,d} - \frac{R_l}{L} I_{L,q} \\ \dot{I}_{td} = -\frac{1}{L_t} V_d - \frac{R_t}{L_t} I_{td} + \omega_0 I_{tq} + \frac{1}{L_t} V_{td} \\ \dot{I}_{tq} = -\frac{1}{L_t} V_q - \omega_0 I_{td} - \frac{R_t}{L_t} I_{tq} + \frac{1}{L_t} V_{tq} \\ \dot{V}_{\mathrm{DC}} = -\frac{3}{2} \frac{I_{td} V_{td}}{C_{\mathrm{DC}} V_{\mathrm{DC}}} - \frac{3}{2} \frac{I_{tq} V_{tq}}{C_{\mathrm{DC}} V_{\mathrm{DC}}} + \frac{1}{C_{\mathrm{DC}}} I_{\mathrm{PV}} \end{cases} \tag{4}$$

where $i_{b,dq}$ and $v_{b,dq}$ are the dq-components of the current delivered by the ESu and of the VSC$_M$ output voltage. Then, the state-space representation of (4) is the following

$$\begin{cases} \dot{x}_1(t) = -\frac{1}{RC} x_1(t) + \omega_0 x_2(t) + \frac{1}{C} x_3(t) - \frac{1}{C} x_5(t) + \frac{1}{C} x_7(t) \\ \dot{x}_2(t) = -\omega_0 x_1(t) - \frac{1}{RC} x_2(t) + \frac{1}{C} x_4(t) - \frac{1}{C} x_6(t) + \frac{1}{C} x_8(t) \\ \dot{x}_3(t) = -\frac{1}{L_b} x_1(t) - \frac{R_b}{L_b} x_3(t) + \omega_0 x_4(t) + \frac{1}{L_b} u_1(t) \\ \dot{x}_4(t) = -\frac{1}{L_b} x_2(t) - \omega_0 x_3(t) - \frac{R_b}{L_b} x_4(t) + \frac{1}{L_b} u_2(t) \\ \dot{x}_5(t) = \frac{1}{L} x_1(t) - \frac{R_l}{L} x_5(t) + \omega_0 x_6(t) \\ \dot{x}_6(t) = \frac{1}{L} x_2(t) - \omega_0 x_5(t) - \frac{R_l}{L} x_6(t) \\ \dot{x}_7(t) = -\frac{1}{L_t} x_1(t) - \frac{R_t}{L_t} x_7(t) + \omega_0 x_8(t) + \frac{1}{L_t} u_3(t) \\ \dot{x}_8(t) = -\frac{1}{L_t} x_2(t) - \omega_0 x_7(t) - \frac{R_t}{L_t} x_8(t) + \frac{1}{L_t} u_4(t) \\ \dot{x}_9(t) = -\frac{3}{2} \frac{x_7(t) u_3(t)}{C_{\mathrm{DC}} x_9(t)} - \frac{3}{2} \frac{x_8(t) u_4(t)}{C_{\mathrm{DC}} x_9(t)} + \frac{1}{C_{\mathrm{DC}}} u_5(t) \\ y_{bd}(t) = x_1(t) \\ y_{bq}(t) = x_2(t) \\ y_{\mathrm{PV}d}(t) = x_9(t) \\ y_{\mathrm{PV}q}(t) = x_8(t) \end{cases} \tag{5}$$

where $x = [V_d\ V_q\ I_{bd}\ I_{bq}\ I_{Ld}\ I_{Lq}\ I_{td}\ I_{tq}\ V_{DC}]^T \in \mathcal{X} \subset \mathbb{R}^9$ is the state variables vector, $u = [V_{bd}\ V_{bq}\ V_{td}\ V_{tq}\ I_{\mathrm{PV}}]^T \in \mathcal{U} \subset \mathbb{R}^5$ is the input vector, and $y_{\mathrm{IOM}} = [V_d\ V_q\ I_{tq}\ V_{\mathrm{DC}}]^T \in \mathbb{R}^4$ is the output vector. The input I_{PV} is assumed to be Lipschitz continuous.

Now, we are in a position to formulate the control problem to solve: *design a robust control strategy able to guarantee that the error between any controlled variable and the corresponding desired value is steered to zero in a finite time even in presence of the uncertainties.*

IV. The Proposed Sliding Mode Control Scheme

In this section, a control scheme based on the sliding mode methodology to solve the aforementioned control problem is discussed. Note that, because of the master-slave architecture, two different controllers need to be designed, i.e., for the ESu and for the PV DGu, respectively.

A. Design of the Sliding Manifold

Consider the master ESu in the state-space model (5). The sliding variables are chosen as the tracking error between the voltage reference value and the actual one [21], [22], i.e.,

$$\sigma_{bd}(t) = y_{bd,\mathrm{ref}} - y_{bd}(t) \tag{6}$$

$$\sigma_{bq}(t) = y_{bq,\mathrm{ref}} - y_{bq}(t) \tag{7}$$

where $y_{bi,\mathrm{ref}}$, $i = d,q$ are assumed to be of class C and with first time derivative Lipschitz continuous. Denote with r the relative degree of the system, i.e., the minimum order r of the time derivative $\sigma_{bi}^{(r)}$, $i = d,q$, of the sliding variable in which the control u explicitly appears. Relying on system (5) and (6), (7), one can observe that r is equal to 2. This implies that a SOSM control can be naturally applied [10], [18].

Now, consider the DC-Link of the PV DGu, and set the sliding variable as

$$\sigma_{\mathrm{PV}d}(t) = y_{\mathrm{PV}d,\mathrm{ref}} - y_{\mathrm{PV}d}(t) \tag{8}$$

$$\sigma_{\mathrm{PV}q}(t) = y_{\mathrm{PV}q,\mathrm{ref}} - y_{\mathrm{PV}q}(t) \tag{9}$$

where $y_{\mathrm{PV}i,\mathrm{ref}}$, $i=d,q$ are assumed to be of class C and with first time derivative Lipschitz continuous. Relying on system (5) and (8), (9), one can observe that r is equal to 1. This implies that a first order sliding mode control naturally applies.

B. Design of the Control Law

The proposed control approaches are hereafter described for the ESu and for the PV DGu.

1) SOSM Voltage Control of ESu: Making reference to the SOSM control theory, define the so-called auxiliary variables as $\xi_{bd,1}=\sigma_{bd}$ and $\xi_{bq,1}=\sigma_{bq}$ such that the corresponding auxiliary systems can be written as

$$\begin{cases}\dot{\xi}_{bi,1}(t)=\xi_{bi,2}(t)\\ \dot{\xi}_{bi,2}(t)=f_{bi}(x(t),u_{\mathrm{PV}}(t))+g_{bi}u_{bi}(t)\end{cases}\qquad i=d,q \quad (10)$$

where u_{bi} are the dq-components of the inverter output voltages, $\xi_{bi,2}$ are assumed to be unmeasurable, and

$$\begin{aligned}f_{bd}(\cdot) &= (\omega_0^2-\tfrac{1}{(RC)^2}+\tfrac{1}{L_bC}+\tfrac{1}{LC}+\tfrac{1}{L_tC})x_1(t)\\ &+\tfrac{2\omega_0}{RC}x_2(t)+(\tfrac{1}{RC^2}+\tfrac{R_b}{L_bC})x_3(t)-\tfrac{2\omega_0}{C}x_4(t)\\ &-(\tfrac{1}{RC^2}+\tfrac{R_l}{LC})x_5(t)+\tfrac{2\omega_0}{C}x_6(t)+(\tfrac{1}{RC^2}+\tfrac{R_t}{L_tC})x_7(t)\\ &-\tfrac{2\omega_0}{C}x_8(t)-\tfrac{1}{L_tC}u_3(t)+\ddot{x}_{1,\mathrm{ref}}(t)\\ f_{bq}(\cdot) &= (\omega_0^2-\tfrac{1}{(RC)^2}+\tfrac{1}{L_bC}+\tfrac{1}{LC}+\tfrac{1}{L_tC})x_2(t)\\ &-\tfrac{2\omega_0}{RC}x_1(t)+\tfrac{2\omega_0}{C}x_3(t)+(\tfrac{1}{RC^2}+\tfrac{R_b}{L_bC})x_4(t)\\ &-\tfrac{2\omega_0}{C}x_5(t)-(\tfrac{1}{RC^2}+\tfrac{R_l}{LC})x_6(t)+\tfrac{2\omega_0}{C}x_7(t)\\ &+(\tfrac{1}{RC^2}+\tfrac{R_t}{L_tC})x_8(t)-\tfrac{1}{L_tC}u_4(t)+\ddot{x}_{2,\mathrm{ref}}(t)\\ g_{bi} &= -\tfrac{1}{L_bC},\quad i=d,q\end{aligned} \quad (11)$$

are allowed to be uncertain but bounded, i.e,

$$\begin{aligned}&|f_{bi}(\cdot)|\le F_{bi}\\ &-G_{bi,M}\le g_{bi}\le -G_{bi,m}<0\end{aligned} \quad (12)$$

F_{bi}, $G_{bi,m}$ and $G_{bi,M}$ being positive known constants. Note that, the existence of bound F_{bi} is verified in real applications. In fact, $f_{bi}(\cdot)$, $i=d,q$, depend on electric signals related to the finite power of the system.

The control laws, which are designed in order to steer $\xi_{bi,1}(t)$ and $\xi_{bi,2}(t)$, $i=d,q$, to zero in a finite time even in presence of the uncertainties, in analogy with [10], are the following

$$u_{bi}(t)=\alpha_{bi}U_{bi,\max}\,\mathrm{sgn}\left(\xi_{bi,1}(t)-\tfrac{1}{2}\xi_{bi,1,\max}\right) \quad (13)$$

with the control parameters chosen so as to satisfy

$$U_{bi,\max}>\max\left(\frac{F_{bi}}{\alpha^*_{bi}G_{bi,m}};\frac{4F_{bi}}{3G_{bi,m}-\alpha^*_{bi}G_{bi,M}}\right) \quad (14)$$

$$\alpha^*_{bi}\in(0,1]\cap\left(0,\frac{3G_{bi,m}}{G_{bi,M}}\right) \quad (15)$$

Remark 1: Note that, in order to alleviate the so-called chattering phenomenon and feed a continuos modulating signal into the photovoltaic inverter, an artificial increment of the relative degree of the system could be performed by applying a third order sliding mode (3-SM) control algorithm analogously to that presented in [21], [22].

2) Unit Vector Sliding Mode Control of PV DGu: In order to design the sliding mode control law for the PV DGu in system (5), selecting the sliding variable as in (8)-(9), one can notice that they are coupled with respect to the control variables u_3 and u_4, i.e.,

$$\dot{\sigma}_{\mathrm{PV}d}(t)=\dot{x}_{9,\mathrm{ref}}+\frac{3}{2}\frac{x_7u_3}{C_{\mathrm{DC}}x_9}+\frac{3}{2}\frac{x_8u_4}{C_{\mathrm{DC}}x_9}-\frac{1}{C_{\mathrm{DC}}}u_5 \quad (16)$$

$$\dot{\sigma}_{\mathrm{PV}q}(t)=\dot{x}_{8,\mathrm{ref}}+\frac{x_2}{L_t}+\omega_0x_7+\frac{R_t}{L_t}x_8-\frac{1}{L_t}u_4 \quad (17)$$

So, a sliding mode control law based on the so-called unit vector approach is introduced. Specifically, let $\sigma_{\mathrm{PV}}=[\sigma_{\mathrm{PV}d},\sigma_{\mathrm{PV}q}]^T$ denote the sliding variables vector, and let $u_{\mathrm{PV}}=[u_3,u_4]^T$ be the control vector. Then the control law can be formulated as follows

$$u_{\mathrm{PV}}=-U_{\max}\frac{\sigma_{\mathrm{PV}}}{\|\sigma_{\mathrm{PV}}\|} \quad (18)$$

where $U_{\max}$ is a positive constant in order to enforce the sliding mode [9].

3) SOSM Control of the PV DGu: Because of the discontinuous nature of the the control law (18), the so-called chattering phenomenon can occur. In order to provide a chattering attenuation, the system relative degree can be artificially increased and a SOSM applies. Also in this case one can define the auxiliary variables $\xi_{\mathrm{PV}d,1}=\sigma_{\mathrm{PV}d}$ and $\xi_{\mathrm{PV}q,1}=\sigma_{\mathrm{PV}q}$ such that the corresponding auxiliary systems result in being

$$\begin{cases}\dot{\xi}_{\mathrm{PV}i,1}(t)=\xi_{\mathrm{PV}i,2}(t)\\ \dot{\xi}_{\mathrm{PV}i,2}(t)=f_{\mathrm{PV}i}(x(t),u_{\mathrm{PV}}(t))+g_{\mathrm{PV}i}(x(t))w_{\mathrm{PV}i}(t)\\ \dot{u}_{\mathrm{PV}i}(t)=w_{\mathrm{PV}i}(t)\end{cases}\qquad i=d,q \quad (19)$$

where $u_{\mathrm{PV}i}$, are the dq-components of the VSC output voltages, $\xi_{\mathrm{PV}i,2}$ are assumed to be unmeasurable, and

$$\begin{aligned}f_{\mathrm{PV}d}(\cdot) &= \tfrac{3}{2}\tfrac{\dot{x}_7(t)x_9(t)u_3(t)}{C_{\mathrm{DC}}x_9^2(t)}-\tfrac{3}{2}\tfrac{x_7(t)\dot{x}_9(t)u_3(t)}{C_{\mathrm{DC}}x_9^2(t)}\\ &+\tfrac{3}{2}\tfrac{\dot{x}_8(t)x_9(t)u_4(t)}{C_{\mathrm{DC}}x_9^2(t)}+\tfrac{3}{2}\tfrac{x_8(t)x_9(t)\dot{u}_4(t)}{C_{\mathrm{DC}}x_9^2(t)}\\ &-\tfrac{3}{2}\tfrac{x_8(t)\dot{x}_9(t)u_4(t)}{C_{\mathrm{DC}}x_9^2(t)}-\tfrac{1}{C_{\mathrm{DC}}}\dot{u}_5(t)+\ddot{x}_{9,\mathrm{ref}}(t)\\ f_{\mathrm{PV}q}(\cdot) &= -\tfrac{2\omega_0}{L_t}x_1(t)-(\tfrac{1}{RL_tC}+\tfrac{R_t}{L_t^2})x_2(t)+\tfrac{1}{CL_t}x_4(t)\\ &-\tfrac{1}{L_tC}x_6(t)-\tfrac{2\omega_0R_t}{L_t}x_7(t)\\ &+(\tfrac{1}{L_tC}+\omega_0^2-\tfrac{R_t^2}{L_t^2})x_8(t)\\ &+\tfrac{\omega}{L_t}u_3(t)+\tfrac{R_t}{L_t^2}u_4(t)+\ddot{x}_{8,\mathrm{ref}}(t)\\ g_{\mathrm{PV}d}(\cdot) &= \tfrac{3}{2}\tfrac{x_7(t)x_9(t)}{C_{DC}x_9^2(t)}\\ g_{\mathrm{PV}q} &= -\tfrac{1}{L_t}\end{aligned} \quad (20)$$

are allowed to be uncertain but bounded, i.e.,

$$
\begin{aligned}
&|f_{\mathrm{PV}i}(\cdot)| \leq F_{\mathrm{PV}i} \\
&0 < G_{\mathrm{PV}d,m} \leq g_{\mathrm{PV}d}(\cdot) \leq G_{\mathrm{PV}d,M} \\
&-G_{\mathrm{PV}q,M} \leq g_{\mathrm{PV}q} \leq -G_{\mathrm{PV}q,m} < 0
\end{aligned} \tag{21}
$$

$F_{\mathrm{PV}i}$, $G_{\mathrm{PV}i,m}$ and $G_{\mathrm{PV}i,M}$ being positive known constants. Note that the sign of $g_{\mathrm{PV}d}$ is always positive since all the terms are greater than zero, which is true for physical reasons. The control laws, designed to steer $\xi_{\mathrm{PV}i,1}(t)$ and $\xi_{\mathrm{PV}i,2}(t)$, $i = d,q$, to zero in a finite time even in presence of the uncertainties, in this second case, can be expressed as follows

$$
\begin{aligned}
w_{\mathrm{PV}d}(t) &= -\alpha_{\mathrm{PV}d} U_{\mathrm{PV}d,\max} \operatorname{sgn}\left(\xi_{\mathrm{PV}d,1}(t) - \tfrac{1}{2}\xi_{\mathrm{PV}d,1\max}\right) \\
w_{\mathrm{PV}q}(t) &= \alpha_{\mathrm{PV}q} U_{\mathrm{PV}q,\max} \operatorname{sgn}\left(\xi_{\mathrm{PV}q,1}(t) - \tfrac{1}{2}\xi_{\mathrm{PV}q,1\max}\right)
\end{aligned} \tag{22}
$$

with bounds

$$
U_{\mathrm{PV}i,\max} > \max\left(\frac{F_{\mathrm{PV}i}}{\alpha^*_{\mathrm{PV}i} G_{\mathrm{PV}i,m}}; \frac{4F_{\mathrm{PV}i}}{3G_{\mathrm{PV}i,m} - \alpha^*_{\mathrm{PV}i} G_{\mathrm{PV}i,M}}\right) \tag{23}
$$

$$
\alpha^*_{\mathrm{PV}i} \in (0,1] \cap \left(0, \frac{3G_{\mathrm{PV}i,m}}{G_{\mathrm{PV}i,M}}\right) \tag{24}
$$

Note that, the discontinuity of the SOSM control laws $w_{\mathrm{PV}i}$, $i = d,q$ only affects $\ddot{\sigma}_{\mathrm{PV}i}$. Then the modulating signal fed into the photovoltaic inverter is continuous.

V. Stability Analysis

With reference to the proposed control algorithms, the following results can be proved.

Lemma 1: The sliding variables $\sigma_{bd}(t)$ and $\sigma_{bq}(t)$, by applying the control laws (13)-(15), are steered to zero in a finite time.

Lemma 2: The sliding variables $\sigma_{\mathrm{PV}d}(t)$ and $\sigma_{\mathrm{PV}q}(t)$, by applying the control laws (18), are steered to zero in a finite time.

Lemma 3: The sliding variables $\sigma_{\mathrm{PV}d}(t)$ and $\sigma_{\mathrm{PV}q}(t)$, by applying the control laws (22)-(24), are steered to zero in a finite time.

Now, let $e = [e_1, \ldots, e_9]^T$ denote the error given by the difference between the state and the equilibrium points associated to the desired value $y_{\mathrm{ref}} = [y_{bd,\mathrm{ref}}, y_{bq,\mathrm{ref}}, y_{\mathrm{PV}d,\mathrm{ref}}, y_{\mathrm{PV}q,\mathrm{ref}}]^T$. With reference to e, the following result can be proved.

Theorem 1: Given system (1)-(5) and the sliding variables (6)-(9) controlled via the SOSM algorithm in (13)-(15) and (22)-(24), $\forall t \geq t_r$, t_r being the time instant when $\sigma_{bd}(t)$, $\sigma_{bq}(t)$, $\sigma_{\mathrm{PV}d}(t)$, $\sigma_{\mathrm{PV}q}(t)$ and $\dot{\sigma}_{bd}(t)$, $\dot{\sigma}_{bq}(t)$, $\dot{\sigma}_{\mathrm{PV}d}(t)$, $\dot{\sigma}_{\mathrm{PV}q}(t)$ are identically zero (i.e., the controlled system features a SOSM), $\forall x(t_r) \in \mathcal{X}$, then the origin of the error system state space is an asymptotically stable equilibrium point.

VI. Case Study

In this section the proposed SM control strategies are verified in simulation by implementing the master-slave model of a microgrid in IOM. It is composed of an energy storage unit (ESu), which serves as master, and of a photovoltaic distributed generation unit (PV DGu), which has the role of slave (see Fig. 1). The electric parameters of the microgrid are reported in Table I.

During simulations, to show the effectiveness of the proposed SM controllers for MPPT of PV inverters, critical unknown dynamics of solar irradiation are considered. In particular, Fig. 2 shows the trapezoidal variations of the DC current I_{PV} generated by the PV arrays. It can be seen from Fig. 3 that, by applying the proposed SOSM control algorithm for MPPT of the PV DGu, the DC-link voltage V_{DC} is maintained constant at the reference value $V_{\mathrm{DC,ref}} = 1000\,\mathrm{V}$. On the other hand, worse performances are obtained if traditional proportional-integral (PI) controllers are used. Note that the gains of PI controllers have been tuned relying on the standard Ziegler-Nichols method [23] to obtain a satisfactory behaviour of the controlled system, given the type of the control law. Moreover, Fig. 3 shows that, by applying the proposed SOSM control algorithm, satisfactory performances are attained also in terms of chattering alleviation with respect to the unit vector approach.

Consequently, by applying PI controllers, because of the impossibility of maintaining the DC-link voltage V_{DC} constant, the voltage of the DGu in IOM is perturbed, as illustrated in Fig. 4.

From the comparison of the PI control, of the unit vector approach and of the SOSM control, the root mean square (RMS) error of V_{DC} results in being equal to $1.1742\,\mathrm{V}$, $0.054\,\mathrm{V}$ and $5.4813 \times 10^{-4}\,\mathrm{V}$, respectively. It is evident that the proposed SM control approaches outperforms the conventional PI controllers.

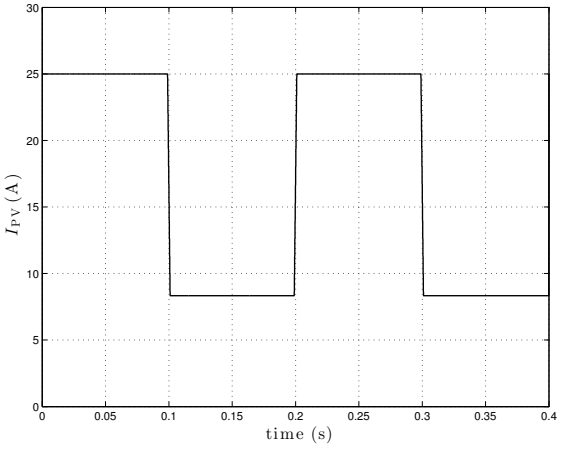

Fig. 2. Time evolution of the DC current I_{PV} generated by PV arrays, which is a model uncertainty.

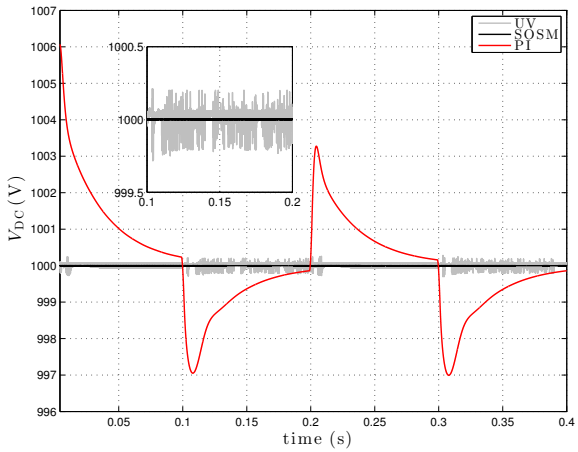

Fig. 3. Time evolution of the DC-link voltage V_{DC} by applying UV, SOSM and PI controllers, in presence of model uncertainties.

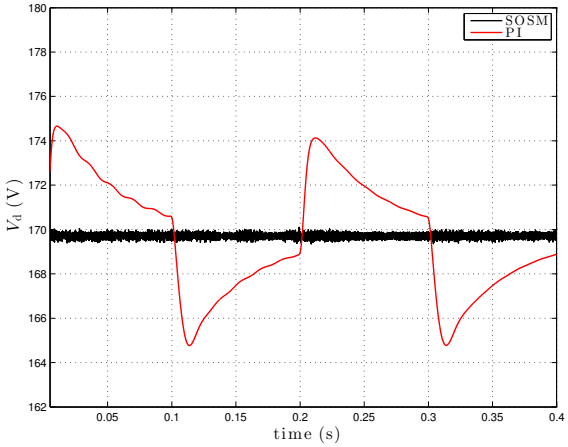

Fig. 4. Time evolution of the direct component of the load voltage by applying SOSM and PI controllers, in presence of model uncertainties.

VII. Conclusions

In this paper the model of a photovoltaic-based microgrid has been introduced. It has been defined in islanded operation mode, including the dynamics of the direct current bus between the photovoltaic arrays and the corresponding inverter. A master-slave configuration with sliding mode controllers has been designed to maintain constant the voltage of the point of common coupling. Specifically, a second order sliding mode control of suboptimal type has been applied to the ESu in order to regulate the voltage of the microgrid, while a first order sliding mode control based on the so-called unit vector approach has been applied to the photovoltaic DGu. A suboptimal second order sliding mode controller has been designed also for the photovoltaic DGu in order to alleviate the so-called chattering phenomenon. The stability properties have been discussed, and the SM controllers have been assessed in simulation with satisfactory performances, also in comparison with respect to conventional PI controllers.

References

[1] R. Lasseter, "Microgrids," in *Power Engineering Society Winter Meeting, 2002. IEEE*, vol. 1, 2002, pp. 305–308 vol.1.

[2] J. Guerrero, P. C. Loh, T.-L. Lee, and M. Chandorkar, "Advanced control architectures for intelligent microgrids - part ii: Power quality, energy storage, and ac/dc microgrids," *IEEE Trans. Ind. Electron.*, vol. 60, no. 4, pp. 1263–1270, Apr. 2013.

[3] M. Babazadeh and H. Karimi, "A robust two-degree-of-freedom control strategy for an islanded microgrid," *IEEE Trans. Power Del.*, vol. 28, no. 3, pp. 1339–1347, Jul. 2013.

[4] D. Sera, T. Kerekes, R. Teodorescu, and F. Blaabjerg, "Improved mppt algorithms for rapidly changing environmental conditions," in *Proc. 12th Int. Power Electron. and Motion Control Conf.*, Aug. 2006, pp. 1614–1619.

[5] R. Kadri, J.-P. Gaubert, and G. Champenois, "An improved maximum power point tracking for photovoltaic grid-connected inverter based on voltage-oriented control," *IEEE Trans. Ind. Electron.*, vol. 58, no. 1, pp. 66–75, Jan. 2011.

[6] I.-S. Kim, "Robust maximum power point tracker using sliding mode controller for the three-phase grid-connected photovoltaic system," *Solar Energy*, vol. 81, no. 3, pp. 405–414, Mar. 2007.

[7] R. Benadli, B. Khiari, and A. Sellami, "Three-phase grid-connected photovoltaic system with maximum power point tracking technique based on voltage-oriented control and using sliding mode controller," in *Proc. 6th Int. Renewable Energy Congress (IREC)*, Mar. 2015, pp. 1–6.

[8] C. Edwards and S. K. Spurgen, *Sliding Mode Control: Theory and Applications*. London, UK: Taylor and Francis, 1998.

[9] V. I. Utkin, *Sliding Modes in Optimization and Control Problems*. New York: Springer Verlag, 1992.

[10] G. Bartolini, A. Ferrara, and E. Usai, "Chattering avoidance by second-order sliding mode control," *IEEE Trans. Automat. Control*, vol. 43, no. 2, pp. 241–246, Feb. 1998.

[11] G. Bartolini, A. Ferrara, E. Usai, and V. Utkin, "On multi-input chattering-free second-order sliding mode control," *IEEE Trans. Automat. Control*, vol. 45, no. 9, pp. 1711–1717, Sep. 2000.

[12] F. Dinuzzo and A. Ferrara, "Higher order sliding mode controllers with optimal reaching," *IEEE Trans. Automat. Control*, vol. 54, no. 9, pp. 2126 –2136, Sep. 2009.

[13] G. Bartolini, A. Ferrara, A. Pisano, and E. Usai, "Adaptive reduction of the control effort in chattering-free sliding-mode control of uncertain nonlinear systems," *Appl. Math. Comput. Sci.*, vol. Vol. 8, no 1, pp. 51–71, 1998.

[14] G. P. Incremona, M. Cucuzzella, and A. Ferrara, "Adaptive suboptimal second-order sliding mode control for microgrids," *International Journal of Control*, pp. 1–19, Jan. 2016.

[15] M. Tanelli and A. Ferrara, "Enhancing robustness and performance via switched second order sliding mode control," *Automatic Control, IEEE Transactions on*, vol. 58, no. 4, pp. 962–974, Apr. 2013.

[16] M. Cucuzzella, G. P. Incremona, and A. Ferrara, "Event-triggered sliding mode control algorithms for a class of uncertain nonlinear systems: Experimental assessment," in *Proc. IEEE American Control Conf.*, Boston, MA, USA, Jul. 2016.

[17] M. Cucuzzella and A. Ferrara, "Event-triggered second order sliding mode control of nonlinear uncertain systems," in *Proc. European Control Conf.*, Aalborg, Denmark, 2016.

[18] G. Bartolini, A. Ferrara, and E. Usai, "Output tracking control of uncertain nonlinear second-order systems," *Automatica*, vol. 33, no. 12, pp. 2203 – 2212, Dec. 1997.

[19] G. Bartolini, A. Ferrara, A. Levant, and E. Usai, *On second order sliding mode controllers*, ser. Lecture Notes in Control and Information Sciences. Springer London, 1999, vol. 247.

[20] M. Cucuzzella, G. P. Incremona, and A. Ferrara, "Master-slave second order sliding mode control for microgrids," in *Proc. IEEE American Control Conf. (ACC)*, Jul. 2015.

[21] M. Cucuzzella, G. Incremona, and A. Ferrara, "Design of robust higher order sliding mode control for microgrids," *Emerging and Selected Topics in Circuits and Systems, IEEE Journal on*, vol. 5, no. 3, pp. 393–401, Sep. 2015.

[22] M. Cucuzzella, G. P. Incremona, and A. Ferrara, "Third order sliding mode voltage control in microgrids," in *Proc. IEEE European Control Conf. (ECC)*, Jul. 2015.

[23] J. G. Ziegler and N. B. Nichols, "Optimum settings for automatic controllers," *ASME. J. Dyn. Sys.*, vol. 64, no. 759, 1942.